

Direct current superconducting quantum interferometers with asymmetric shunt resistors

M. Rudolph,¹ J. Nagel,¹ J.M. Meckbach,² M. Kemmler,¹ M. Siegel,² K. Ilin,² D. Koelle,¹ and R. Kleiner^{1,*}

¹*Physikalisches Institut – Experimentalphysik II and Center for Collective Quantum Phenomena in LISA⁺,
Universität Tübingen, Auf der Morgenstelle 14, D-72076 Tübingen, Germany*

²*Institut für Mikro- und Nanoelektronische Systeme,
Karlsruhe Institute of Technology, Hertzstr. 16, D-76187 Karlsruhe, Germany*

We have investigated asymmetrically shunted Nb/Al-AlO_x/Nb direct current (dc) superconducting quantum interference devices (SQUIDs). While keeping the total resistance R identical to a comparable symmetric SQUID with $R^{-1} = R_1^{-1} + R_2^{-1}$, we shunted only one of the two Josephson junctions with $R = R_{1,2}/2$. Simulations predict that the optimum energy resolution ϵ and thus also the noise performance of such an asymmetric SQUID can be 3–4 times better than that of its symmetric counterpart. Experiments at a temperature of 4.2 K yielded $\epsilon \approx 32 \hbar$ for an asymmetric SQUID with an inductance of 22 pH. For a comparable symmetric device $\epsilon = 110 \hbar$ was achieved, confirming our simulation results.

PACS numbers: 85.25.CP, 85.25.Dq, 74.25.F- 74.40.De

The transport characteristics and noise performance of direct current (dc) superconducting quantum interference devices SQUIDs having symmetric Josephson junctions has been intensively studied from the 1970's. Numerical simulations of the Langevin equations describing the SQUID dynamics reliably helped to understand the modulation patterns $V(\Phi_a, I)$ and the low-frequency voltage noise power $S_V(\Phi_a, I)$, where V is the dc voltage across the SQUID, I is the bias current and Φ_a is the applied flux. With the flux-to-voltage transfer function $V_\Phi = |dV/d\Phi_a|$, one obtains the flux noise power $S_\Phi = S_V/V_\Phi^2$ or energy resolution $\epsilon = S_\Phi/2L$, where L is the SQUID inductance. For an optimized device one obtains in the limit of small thermal fluctuations an energy resolution $\epsilon = (8 - 9)k_B T L/R$ for an inductance parameter $\beta_L = 2I_0 L/\Phi_0$ somewhat below 1 [1, 2]. Here, I_0 and R respectively denote the junction critical current and resistance. Φ_0 is the flux quantum. Although ϵ can be very low – for example, in Ref. 3 a value of $\sim 3 \hbar$ has been reported at 4.2 K for a 2 pH device – one may ask whether or not it still can be improved by introducing asymmetries in the junction parameters or perhaps by adding new elements to the SQUID. Early simulations have shown that asymmetries in the junction critical currents and resistances can enhance V_Φ , although for the prize of asymmetric $V(\Phi_a)$ patterns [1]. It has also been predicted that an additional damping resistor can enhance V_Φ [4, 5]. Several works addressed junction asymmetries and additional damping resistors in more detail [6–11], with the result that the transfer function can be increased and flux noise be decreased. The above investigations, however, explored only a very limited range of parameters and often addressed devices where the symmetric counterpart was far from optimum.

Let us start with a theoretical analysis, using the stan-

dard Langevin equations [1] where the Josephson junctions are described by the resistively and capacitively shunted junction model[12, 13]. With $i = I/I_0$ the normalized currents through the junctions $k = 1, 2$ are given by

$$\frac{i}{2} \pm j = \beta_c(1 \pm \alpha_c) \dot{\delta}_k + (1 \pm \alpha_r) \dot{\delta}_k + (1 \pm \alpha_i)(\Phi) \sin(\delta_k) + i_{N,k} \quad (1)$$

, α_c , α_r and α_i denote the asymmetries in capacitance, resistance and critical current respectively. The junction critical currents are $I_{0,k} = I_0(1 \pm \alpha_i)$, their resistances $R/(1 \pm \alpha_r)$ and their capacitances $C_k = C(1 \pm \alpha_c)$. ‘ \pm ’ refers to junctions 1 and 2, respectively. δ_k denotes the phase of junction k , $j = J/I_0$ is the normalized circulating current in the SQUID loop and $\beta_c = 2\pi I_0 R^2 C/\Phi_0$ is the Stewart-McCumber parameter. Dots denote derivative with respect to normalized time $\tau = \Phi_0/2\pi I_0 R$. The normalized noise current $i_{N,k}$ has a spectral power density 4Γ , with $\Gamma = 2\pi k_B T/I_0 \Phi_0$. The δ_k are related by

$$\delta_2 - \delta_1 = 2\pi\Phi/\Phi_0 + \pi\beta_L(j + \frac{\alpha_L}{2}i) \quad (2)$$

where Φ is the total flux through the SQUID. $L = L_1 + L_2$, where L_1 and L_2 are the inductances of the two SQUID arms, related to the inductance asymmetry α_L via $L_k = L(1 \pm \alpha_L)/2$.

From Eqs. (1) and (2) one obtains the normalized dc voltage $v = V/I_0 R$, and thus the current voltage characteristic (IVC) by taking the time average of $u = (\dot{\delta}_1 + \dot{\delta}_2)/2$. From a Fourier transform of u one obtains the normalized correlation functions $s_v = S_V 2\pi I_0 R/\Phi_0^3$, $s_\phi = S_\Phi I_0 R/(2\Phi_0 k_B T)$ and $e = s_\phi/2\Gamma\beta_L$.

The quantity we are interested in most is the optimized normalized energy resolution e_{opt} , where optimization is done for some or even all SQUID parameters. Recently, we have performed a systematic optimization of the noise performance of the rf SQUID, optimizing all of its parameters [14, 15]. We now apply the same procedure

* kleiner@uni-tuebingen.de

to fully optimize e of the dc SQUID, with respect to i , $\phi_a = \Phi_a/\Phi_0$, β_L , β_c , α_i , α_c and α_r , i.e., for a given value of one or some of these parameters we find all others so that e_{opt} is minimized. The inductance asymmetry α_L does not appear in the above list, since, for a given bias current, it only causes a phase shift in $v(\phi_a)$ and also the noise correlation functions. Since in practice the junction capacitance is always nonzero, the McCumber parameter β_c should be as large as possible to obtain large values of I_0R . It turns out that β_c values below 0.8 are uncritical in the sense that the other parameters can be tuned so that e_{opt} attains its minimum value irrespective of β_c .

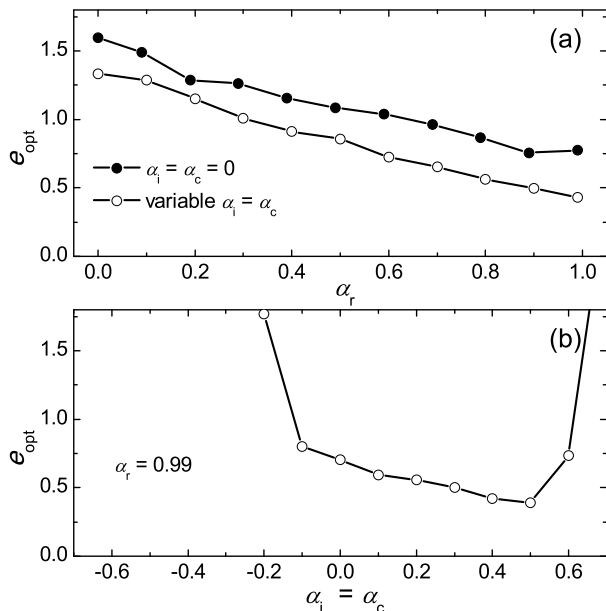


FIG. 1. Optimized normalized energy resolution e_{opt} vs. (a) resistance asymmetry α_r and (b) junction critical current and capacitance asymmetry $\alpha_i = \alpha_c$. Fixed parameters are $\Gamma = 0.01$ and $\beta_c = 0.7$. For all data points β_L has been varied.

Fig. 1(a) shows e_{opt} vs. α_r for $\alpha_i = \alpha_c = 0$ (full circles) and for variable $\alpha_i = \alpha_c$ (open circles). Fixed parameters are $\beta_c = 0.7$ and $\Gamma = 0.01$. The parameters i , ϕ_a and β_L have been varied to minimize e . We have used $\alpha_i = \alpha_c$, having in mind junctions where both I_0 and C scale with the junction area and R can be chosen independently by shunting. The value for Γ was chosen as typical for operation at 4.2 K. For $\alpha_i = 0$, e_{opt} vs. α_r decreases from ~ 1.6 to 0.7 for $\alpha_r \rightarrow 1$. In case of variable α_i the minimum e_{opt} is about 0.4, i.e., a factor of 4 lower than the energy resolution of a comparable symmetric SQUID. Note that each point in the graph corresponds to different values of i , ϕ_a , β_L . We do not list the value of these parameters explicitly but note that in all cases β_L was in the range $0.4 - 0.5$. $\alpha_i = \alpha_c \approx 0.3 - 0.5$ was found in case these parameters were varied.

In Fig. 1(b) we show e_{opt} vs. $\alpha_i = \alpha_c$ for variable β_L and fixed $\beta_c = 0.7$ and $\Gamma = 0.01$ and $\alpha_r = 0.99$. The lowest values of e_{opt} are achieved for α_i near 0.5. For lower

values of α_i , e_{opt} monotonically increases. In particular e_{opt} is achieved when α_i and α_r have the same sign, i.e., the junction having the *lower* resistance should have the *higher* I_0 . We have obtained similar results, giving almost the same lowest values for e_{opt} , also for higher values of Γ (up to 0.1). e_{opt} is thus a robust quantity.

In dimensioned units $\epsilon = e \cdot 2\Phi_0 k_B T / I_0 R$. To maximize I_0 for $\beta_L \approx 0.5$, L should be as small as possible. Then, to maximize R and keep β_c below 1, C should be as small as possible, which for a given capacitance per area means to keep the junction area as small. If junction asymmetries are considered, given a constant critical current density, the size of the weaker junction is presumably limited by the fabrication process and, to obtain an α_i of, e.g., 0.3, the average junction area is increased by about 40% from its minimum value. This basically compensates the gain in e_{opt} . Asymmetries in α_i are thus not necessarily helpful. Thus, below we discuss an experimental design having $\alpha_i = \alpha_c = 0$.

We also note that for α_r very close to 1, e_{opt} increases slightly again with increasing α_r for $\alpha_i = \alpha_c = 0$. This is related to chaotic dynamics which appears in some ranges of i and ϕ_a . Below, we will address this issue in comparison to experimental data. Nonetheless, if small values of e_{opt} can be retained for $\alpha_r \rightarrow 1$, the easiest way to realize the corresponding SQUID experimentally is to “move” the shunt from junction 1 to junction 2, leaving junction 1 unshunted and junction 2 shunted with a resistance $R/2$. In the following we discuss the performance of such a Nb/Al-AlO_x/Nb SQUID and compare it to simulations, as well as to the performance of a corresponding symmetric SQUID.

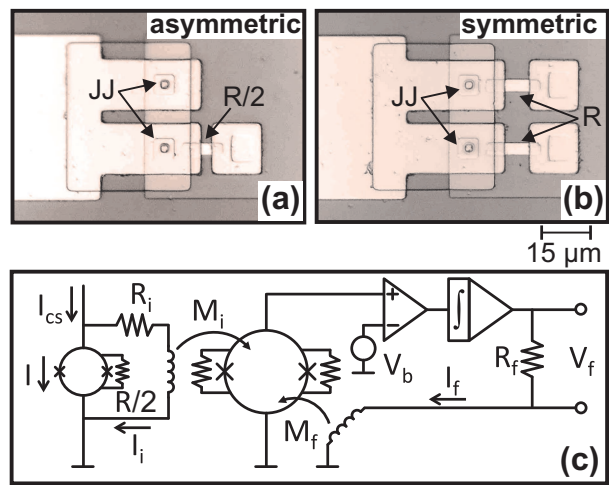


FIG. 2. (Color online) Optical image of the (a) asymmetric and (b) symmetric SQUID. The Josephson junctions are labeled by “JJ” and the shunt resistors by R and $R/2$. (c) Readout scheme of the asymmetric SQUID using a SQUID amplifier operated in flux-locked loop.

Figs. 2(a) and (b) show optical images of an asymmetric and a symmetric SQUID. The SQUIDs have been fabricated using a Nb/Al-AlO_x/Nb technology based on op-

tical photolithography. By a combination of reactive ion etching (RIE) employing CF_4 and O_2 and ion beam etching (IBE) the ground-electrode was defined. The subsequent definition of the junction area was done by RIE and anodic oxidation in an aqueous solution of $(\text{NH}_4)\text{B}_5\text{O}_8$ and $\text{C}_2\text{H}_6\text{O}_2$. Before the definition of the vias (RIE - IBE) the connecting bridges for the anodization between the individual SQUIDs were removed. The following definitions of the resistor, insulation layer and wiring layer were all done using a lift-off technique. For the resistor material a 76 nm thick Palladium layer was deposited, resulting in a sheet resistance of $1 \Omega/\text{sq}$ at $T = 4.2\text{K}$. The ~ 300 nm thick SiO insulation layer was deposited using thermal evaporation while the samples were mounted on a water cooled copper plate ($T_{\text{process}} \leq 26^\circ\text{C}$). After in-situ pre-cleaning, the final Nb wiring layer connecting the junctions, vias and shunt-resistors was dc-magnetron sputtered at room temperature.

Transport and noise measurements were performed at $T = 4.2\text{K}$ in a magnetically and electrically shielded environment. Dc characteristics (I_V , $V(\Phi_a)$, critical current $I_c(\Phi_a)$) were measured in a standard four-point configuration, using low noise current sources and a high impedance room temperature voltage amplifier (RTA). For the noise measurements the RTA was not sensitive enough. Thus, V was preamplified with a commercial SQUID amplifier [16] having a $60 \text{ pV}/\text{Hz}^{1/2}$ resolution, operated in a flux-locked loop with ac flux bias at modulation frequency $f_{\text{mod}} = 256 \text{ kHz}$. The SQUIDs were operated open loop at fixed I and Φ_a . V was measured by connecting the input coil of the SQUID amplifier in parallel to the SQUID. A 5Ω resistor R_i was in series to the input coil, as shown in Fig. 2(c). Due to the low input impedance of the amplifier, the current I_{cs} from the current source divides into I and the current I_i through the input coil. At given I_{cs} , I varies when changing Φ_a , affecting V_Φ and thus the determination of the energy resolution. Using Kirchhoff's laws and the condition for flux-locked loop operation, $I_i M_i = I_f M_f$, with M_i (M_f) being the mutual inductance between the amplifier SQUID and the input (feedback) coil, one obtains $I_i = (M_f/M_i)(V_f/R_f)$. Since M_i , M_f and R_f are constants, I_i can be determined by measuring V_f . To determine $V(\Phi_a)$ for constant I a software control-loop was implemented adjusting I_{cs} such that, for each value of Φ_a , $I = I_{cs} - I_i$ was fixed. The ratio (M_i/M_f) slightly differed for different samples and was adjusted for each device until the bias corrected $V(\Phi_a)$ curve measured with the SQUID amplifier fitted the corresponding $V(\Phi_a)$ curve measured with the RTA; all other measurements for a given device were then performed with fixed (M_f/M_i) .

Fig. 3 (a) shows IVCs of the asymmetric SQUID. Solid black line is for $\Phi_a = 0$, solid gray line for $\Phi_a = 0.5 \Phi_0$. The critical current is $I_c \approx 2I_0 = I_{01} + I_{02} = 62.0 \mu\text{A}$ and for $R/2$ we obtain 0.57Ω , yielding $I_c R = 35.3 \mu\text{V}$. One notes that, in contrast to IVCs of symmetric devices, the IVC of the asymmetric SQUID exhibits several structures, including regions of negative differential resis-

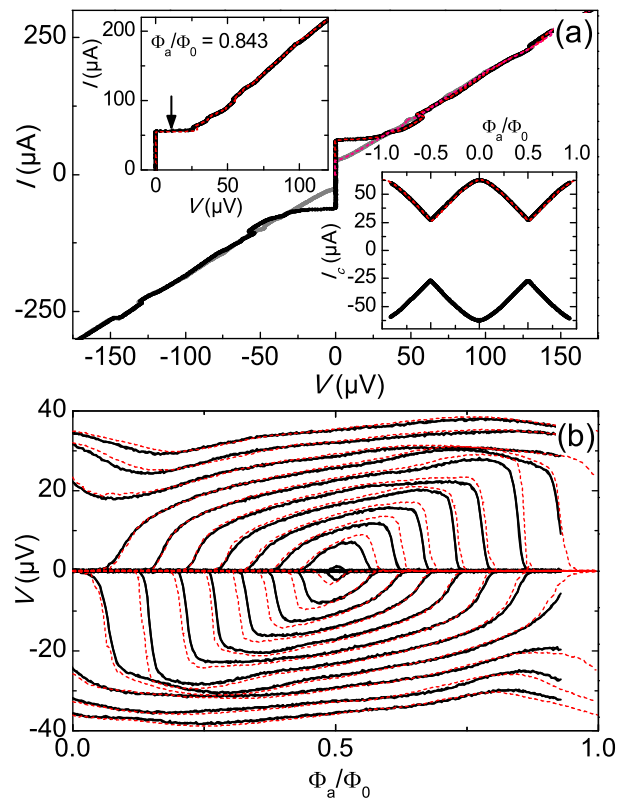


FIG. 3. (Color online) Dc characteristics of the asymmetric SQUID: (a) IVCs at $\Phi_a = 0$ (solid black line) and at $\Phi_a = 0.5 \Phi_0$ (solid gray line). Lower right inset: $I_c(\Phi_a)$. Upper left inset: IVC at $\Phi_a = 0.843 \Phi_0$. The arrow indicates the voltage for the lowest energy resolution. Theoretical curves are shown by dashed lines. (b) $V(\Phi_a)$ (solid black line), for $I = -76.4 \mu\text{A} \dots 75.9 \mu\text{A}$ (in $4.9 \mu\text{A}$ steps). Corresponding theoretical curves are shown by dashed lines.

tance. These structures are reproduced in simulations, cf. dashed lines. The negative differential resistance in fact separates a high-current regime having chaotic dynamics from a more stable low-current regime. For the simulation we have used parameters $\beta_L = 0.675$, $\beta_c = 0.27$, $\Gamma = 0.0065$, $\alpha_r = 0.999$, $\alpha_i = \alpha_c = 0$. These parameters have been inferred partly by fitting the IVC, but also by fitting $I_c(\Phi_a)$. The corresponding data for $I_c(\Phi_a)$ are shown by solid black lines in the lower right inset of Fig. 3 (a). The dashed line in this graph shows the calculated curve. Finally, from β_L and I_0 we obtain $L = 21.7 \text{ pH}$ which is close to the design value of 23.9 pH . The upper left inset of Fig. 3 (a) shows by solid black line the IVC taken at $\Phi_a = 0.843 \Phi_0$. For this particular flux value the best energy resolution was found at the voltage indicated by the arrow. The dashed line is a calculated curve, using the parameters given above. A family of curves $V(\Phi_a)$ for variable I is shown in Fig. 3(b). Experimental data, for different I are shown by solid black lines. The corresponding calculated curves, shown by dashed lines, fit the data reasonably well, showing that the dc characteristics of our device can be understood by the SQUID Langevin

equations. In the $V(\Phi_a)$ curves one notes that the slope $dV/d\Phi_a$ is very steep for $\Phi_a \geq 0.5\Phi_0$, in fact reaching maximum values of about $1.2 \text{ mV}/\Phi_0$ near $I = 56 \mu\text{A}$.

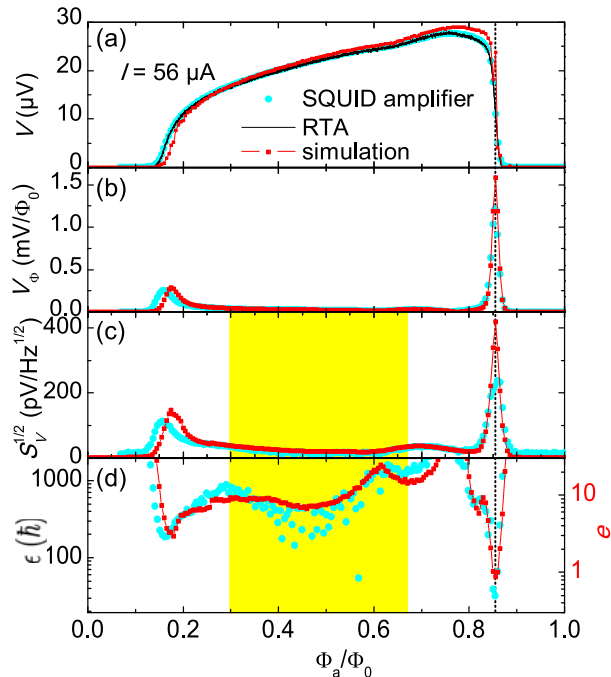


FIG. 4. (Color online) Electric transport and noise vs. Φ_a for the asymmetric SQUID at optimum $I = 56 \mu\text{A}$, measured with SQUID amplifier (dots) in comparison with numerical simulations (line plus symbol): (a) Voltage across the SQUID; solid black line shows corresponding curve measured with a high impedance room temperature amplifier. (b) Transfer function $V_\Phi = dV/d\Phi_a$. (c) Voltage noise $S_V^{1/2}$, experimental data averaged between $100 \text{ Hz} \leq f \leq 3 \text{ kHz}$ (white noise regime). (d) Absolute (left) and normalized (right) energy resolution. In (c) and (d) the noise of the SQUID amplifier has been subtracted; within the shaded area the SQUID amplifier noise was above the noise of the asymmetric SQUID, resulting in large errors when calculating ϵ and e . The vertical dotted line indicates the position of minimum ϵ .

Our central results are shown in Fig. 4. Figure 4(a) shows $V(\Phi_a)$ for the optimum bias current of $56 \mu\text{A}$. Dots represent the experimental data, as taken by the SQUID amplifier. For comparison the solid black line represents the corresponding data taken by the RTA. The two curves are well on top of each other, justifying our method of correcting the bias current in measurements using the SQUID amplifier. The line with symbols is the

theoretical curve obtained from numerical simulations, which agrees well with the experimental curves. Figure 4(b) and (c), respectively, show by dots the experimental V_Φ and the white voltage noise $S_V^{1/2}$, and in comparison the corresponding calculated curves (lines plus symbols). For experimental data, $S_V^{1/2}$ has been averaged between $100 \text{ Hz} \leq f \leq 3 \text{ kHz}$. The voltage noise of the SQUID amplifier has been subtracted. Figure 4(d) displays ϵ and e , calculated from the graphs shown in (b) and (c). For this device the optimum energy resolution is $32 \hbar$; in normalized units, $e_{\text{opt}} = 0.52$. Surprisingly, the theoretical value for $e_{\text{opt}} = 0.85$ is higher. The reason for this is an instability in the calculations, appearing as a chaotic switching between two nearby voltage states [17]. This seems to be absent in the experimental device. The minimum rms flux noise was $133 n\Phi_0/\text{Hz}^{1/2}$ which is also quite low. For comparison, for the symmetric SQUID having parameters $I_0 R = 37.07 \mu\text{V}$, $\beta_L = 0.74$, $\beta_c = 0.18$ and $\Gamma = 0.00526$ we obtained $\epsilon_{\text{opt}} = 110 \hbar$ ($e_{\text{opt}} = 1.79$) and $S_\Phi^{1/2} = 361 n\Phi_0/\text{Hz}^{1/2}$, i.e., a factor of 3.4 higher ϵ_{opt} than for our asymmetric device. Further note that for the asymmetric SQUID β_c was only 0.27, allowing in principle to increase R by a factor of ~ 1.5 , potentially decreasing ϵ to $\sim 20 \hbar$.

In conclusion we have shown that asymmetries in the junction parameters of a dc SQUID can help to significantly improve its noise performance over a SQUID with symmetric junctions. The most practical way to achieve this is to leave one junction unshunted while the other junction is shunted by half of the resistance of the shunts of a symmetric device. Experimentally, we have found a factor of 3.4 improvement of the SQUID energy resolution over a symmetric device with comparable parameters. At least in simulations the drawback of the asymmetric shunt is to introduce chaotic behavior of the SQUID for certain regimes of bias current and applied flux. Our experimental device seems to be less sensitive to chaos. Thus, the asymmetrically shunted SQUID may be useful for applications where ultra-low values of energy resolutions are desired.

ACKNOWLEDGMENTS

This work was supported by the European Research Council via ERC advanced grant SOCATHES, by the DFG via SFB/TRR 21 and in part by the DFG Centre of Functional Nanostructures Project N° B1.5. J. Nagel acknowledges support by the Carl-Zeiss-Stiftung.

- [1] C. D. Tesche and J. Clarke, *J. Low Temp. Phys.* **29**, 301 (1977).
 [2] J. J. P. Bruines, V. J. de Waal, and J. E. Mooij, *J. Low Temp. Phys.* **46**, 383 (1982).

- [3] D. J. Van Harlingen, R. H. Koch, and J. Clarke, *Appl. Phys. Lett.* **41**, 197 (1982).
 [4] K. Enpuku, K. Sueoka, K. Yoshida, and F. Irie, *J. Appl. Phys.* **57**, 1691 (1985).

- [5] K. Enpuku, T. Muta, K. Yoshida, and F. Irie, *J. Appl Phys.* **58**, 1916 (1985).
- [6] R. Kleiner, D. Koelle, F. Ludwig, E. Dantsker, A. H. Miklich, and J. Clarke, *J. Appl. Phys.* **79**, 1129 (1996).
- [7] J. Müller, S. Weiss, R. Gross, R. Kleiner, and D. Koelle, *IEEE Trans. Appl. Phys.* **11**, 921 (2001).
- [8] G. Testa, E. Sarnelli, S. Pagano, C. R. Calidonna, and M. M. Furnari, *J. Appl. Phys.* **89**, 5145 (2001).
- [9] G. Testa, S. Pagano, E. Sarnelli, C. R. Calidonna, and M. M. Furnari, *Appl. Phys. Lett.* **79**, 2943 (2001).
- [10] G. Testa, C. Granata, C. DiRusso, S. Pagano, M. Russo, and E. Sarnelli, *Appl. Phys. Lett.* **79**, 3989 (2001).
- [11] F. Kahlmann, W. E. Booij, M. G. Blamire, P. F. McBrien, N. H. Peng, C. Jeynes, E. J. Romans, C. M. Pegrum, and E. J. Tarte, *IEEE Trans. Appl. Phys.* **11**, 916 (2001).
- [12] W. C. Stewart, *Appl. Phys. Lett.* **12**, 277 (1968).
- [13] D. E. McCumber, *J. Appl. Phys.* **39**, 3113 (1968).
- [14] R. Kleiner, D. Koelle, and J. Clarke, *J. Low Temp. Phys.* **149**, 230 (2007).
- [15] R. Kleiner, D. Koelle, and J. Clarke, *J. Low Temp. Phys.* **149**, 261 (2007).
- [16] SQ100 LTS dc SQUID, PC-100 Single-Channel dc SQUID Electronics System, STAR Cryoelectronics, USA.
- [17] I. Goldhirsch, Y. Imry, G. Wasserman, and E. Ben-Jacob, *Phys. Rev. B* **29**, 1218 (1984).